PLANT SCIENCE

NLR immune receptor–nanobody fusions confer plant disease resistance

Jiorgos Kourelis†, Clemence Marchal†, Andres Posbeyikian, Adeline Harant, Sophien Kamoun*

Plant pathogens cause recurrent epidemics, threatening crop yield and global food security. Efforts to retool the plant immune system have been limited to modifying natural components and can be nullified by the emergence of new pathogen strains. Made-to-order synthetic plant immune receptors provide an opportunity to tailor resistance to pathogen genotypes present in the field. In this work, we show that plant nucleotide-binding, leucine-rich repeat immune receptors (NLRs) can be used as scaffolds for nanobody (single-domain antibody fragment) fusions that bind fluorescent proteins (FPs). These fusions trigger immune responses in the presence of the corresponding FP and confer resistance against plant viruses expressing FPs. Because nanobodies can be raised against most molecules, immune receptor–nanobody fusions have the potential to generate resistance against plant pathogens and pests delivering effectors inside host cells.

Plants lack an adaptive immune system and rely on innate immune receptors to detect invading pathogens. Efforts to retool the plant immune system to design new-to-nature biochemical activities have been largely limited to modification of natural components, for instance through receptor mutagenesis or domain shuffling (*1*–*8*). Although these approaches have yielded promising results, they often target a specific pathogen isolate and thus lack plasticity and adaptability to a wider range of pathogens and pests. Additionally, plant pathogens are notorious for rapidly evolving virulent races that can nullify new resistance specificities. Thus, there is a need for an adaptative system where resistance can be bioengineered as required to target the pathogen genotypes associated with plant disease outbreaks.

One class of immune proteins that could be optimal templates for receptor bioengineering is the subset of intracellular nucleotide-binding, leucine-rich repeat immune receptors (NLRs) that carry unconventional integrated domains (IDs) (*9*–*12*). These IDs are generally thought to mediate pathogen effector detection, either by directly binding to effectors or by acting as a substrate for their enzymatic activity. This activity is subsequently translated into an immune response (*13*–*17*). Often these ID-containing NLRs (NLR-IDs) are genetically linked to conventional NLRs that are required for immune activation after effector detection (*9*, *18*). Pik-1 and Pik-2 are such an NLR receptor pair from rice carrying an N-terminal coiled-coil (CC) domain (*19*). Pik-1 carries an integrated heavy metal–associated (HMA) domain between its CC and the central NB-ARC (nucleotide-binding domain shared with APAF-1, various R proteins, and CED-4) domains that directly binds AVR-Pik effector proteins (avirulence factors) secreted by the blast fungus, *Magnaporthe oryzae* (*13*, *16*, *20*–*24*). AVR-Pik binding to the Pik-1 HMA domain results in Pik-2–dependent immunity (*16*, *19*). The integrated HMA domain of Pik-1 can be mutated or swapped for similar HMA domains to confer recognition of different AVR-Pik alleles (*5*, *25*, *26*). The Pik NLR gene pair has a variety of alleles (such as Pikp, Pikm, Pikh, Piks, and Pik*) that provide immunity to blast isolates expressing different AVR-Pik variants (*27*).

What would be the ultimate ID for engineering made-to-order plant immune receptors? Given that animal adaptive immunity has the capacity to generate antibodies against virtually any antigen that it is exposed to, we reasoned that harnessing antibodies for plant immunity would potentially enable building receptors that respond to a wide range of plant pathogen molecules. We focused on the minimal antigen-binding fragment of single-domain heavy-chain antibodies (known as VHHs or nanobodies) of camelid mammals (*28*–*31*) because they are small, soluble 10- to 15-kDa domains, which tend to correctly fold intracellularly and have many useful properties for biotechnological applications. To test our idea, we generated orthogonal Pik-1 sensors in which the integrated HMA domain is swapped with nanobodies that bind either green fluorescent protein (GFP) or mCherry (*32*–*34*) (Fig. 1, A and B, and table S1). We hypothesized that the engineered versions of Pik-1 would trigger immunity in the presence of GFP or mCherry.

Pikobodies are functional NLR-nanobody fusions

Mutations in the Pik-1 HMA domain often lead to autoimmune activities in the absence of a ligand, and like the immune signaling in response to effector recognition, this activity is dependent on the presence of Pik-2 (*23*, *25*, *26*, *35*). Hence, we first tested whether the Pikm-1–nanobody fusions induce autoimmunity in the presence of Pik-2. Of the 11 tested Pikm-1–nanobody fusions, six did not exhibit autoimmunity when expressed with Pikm-2 in leaves of the model plant *Nicotiana benthamiana* (fig. S1 and table S2), which indicated that they can be used for follow-up gain-of-function assays. Next, we co-expressed 10 Pikm-1–nanobody fusions with GFP or mCherry. Among these, four produced a hypersensitive cell death response (HR, immune response readout) specifically when expressed with their matching fluorescent proteins (FPs) (Enhancer, LaG-16, LaM-4, and LaM-8) (Fig. 1C, fig. S1, and table S2). The response levels were similar to those obtained with a natural combination of Pikm and a blast fungus effector (Fig. 1C and fig. S1). Additionally, a further three fusions that displayed weak autoimmunity gave a stronger HR only when combined with their matching FPs (LaG-24, LaM-2, and LaM-6) (Fig. 1C and fig. S1). This indicates that the Pikm-1–nanobody fusions are functional and can be endowed with new-to-nature activities. We coined the term Pikobody for the combination of Pikm-2 with the engineered Pikm-1–nanobody fusions (Fig. 1).

We reasoned that nanobody aggregation or misfolding upon intracellular expression (*32*) could explain the observed autoactivity (Fig. 1C and fig. S1). We introduced previously described stabilizing nanobody mutations (*32*) in LaG-24, LaM-2, LaM-3, and LaM-6 and found that they abolished Pikobody autoactivity (fig. S2). Three of these Pikobodies carrying the stabilized mutants of LaG-24, LaM-3, and LaM-6 retained the capacity to trigger HR in the presence of the matching FP, whereas LaM-2 did not (fig. S2). This shows that Pikobody autoactivity can be abolished by engineering the core structural features of the nanobodies.

Given that Enhancer and LaM-4 are widely used nanobodies recognizing GFP and mCherry, respectively, we selected Pikobody^{Enhancer} (consisting of Pikm-2 together with the Pikm-1^{Enhancer}–nanobody fusion) and Pikobody$^{LaM\text{-}4}$ (consisting of Pikm-2 together with the Pikm-1$^{LaM\text{-}4}$–nanobody fusion) to further confirm our results. Some pathogen effectors may not be recognized by Pikobodies, for example by having a subcellular localization that precludes recognition. We noted that Pikobody^{Enhancer} and Pikobody$^{LaM\text{-}4}$ specifically responded to three pathogen effectors only when they were tagged with the matching GFP or enhanced GFP (EGFP) or the matching mCherry or mRFP1 (fig. S3 and table S2). This further confirmed that the Pikobodies are functional FP sensors that detect FPs even when they are fused to pathogen effector proteins.

We investigated the extent to which Pikobodies function through similar mechanisms

The Sainsbury Laboratory, University of East Anglia, Norwich Research Park, Norwich NR4 7UH, UK.
*Corresponding author. Email: sophien.kamoun@tsl.ac.uk
†These authors contributed equally to this work.

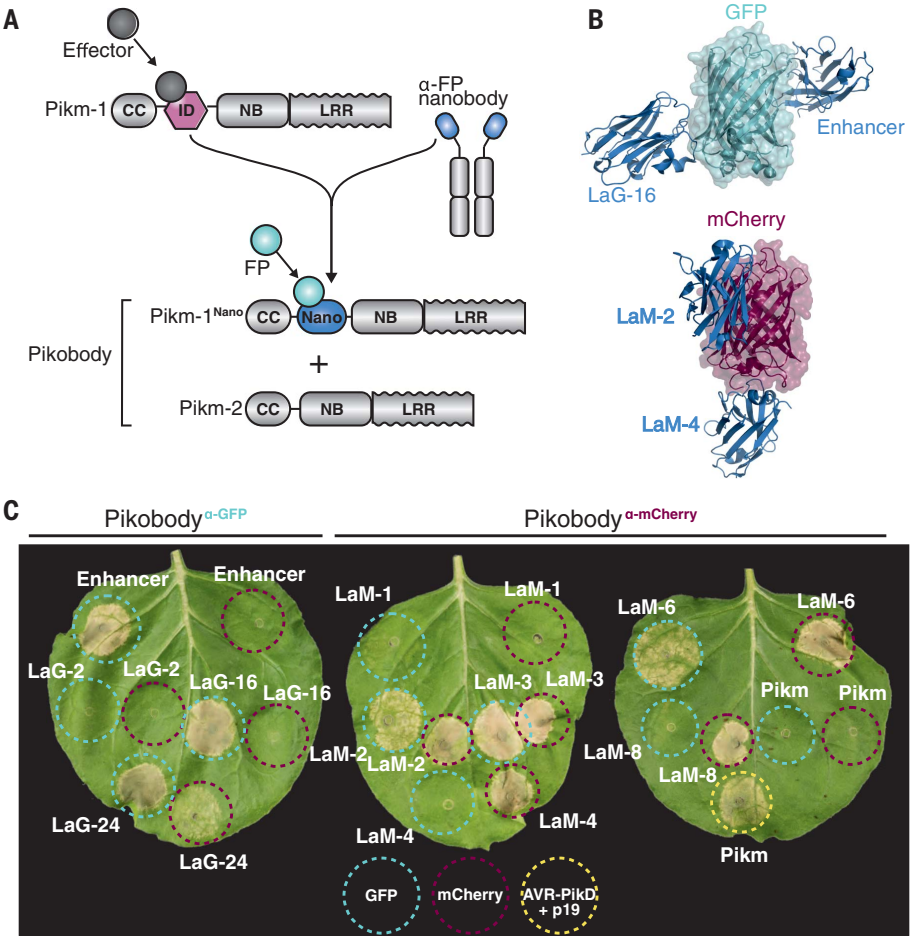

Fig. 1. NLR immune receptor–nanobody fusions trigger a HR in the presence of the corresponding FP antigen. (**A**) Bioengineering of a FP-activated NLR sensor. The integrated HMA domain of the NLR Pikm-1, which is involved in pathogen effector recognition by direct binding, was swapped with nanobodies binding either GFP or mCherry. We coined the term Pikobody for the combination of Pikm-2 with Pikm-1–nanobody fusions. CC, coiled-coil domain; NB, nucleotide-binding domain; LRR, leucine-rich repeat; Nano, nanobody. (**B**) Structures of GFP (cyan) or mCherry (magenta) with the GFP-binding nanobodies Enhancer [Protein Data Bank (PDB) ID: 3K1K] (*33*) and LaG-16 (PDB: 6LR7) (*51*) or the mCherry-binding nanobodies LaM-2 (PDB: 6IR2) and LaM-4 (PDB: 6IR1) (*52*), respectively (dark blue). (**C**) Screen for GFP or mCherry recognition by bioengineered Pikobody$^{\alpha\text{-GFP}}$ or Pikobody$^{\alpha\text{-mCherry}}$ resulting in induction of a HR upon coexpression in *N. benthamiana*. Representative *N. benthamiana* leaves were infiltrated with the indicated constructs and photographed 5 days after infiltration (see fig. S1 for quantification). Cyan and magenta dashed circles indicate GFP or mCherry co-infiltration, respectively. The Pikm pair (Pikm-1 and Pikm-2) co-infiltrated with AVR-PikD, and p19 was used as a positive control for HR (yellow).

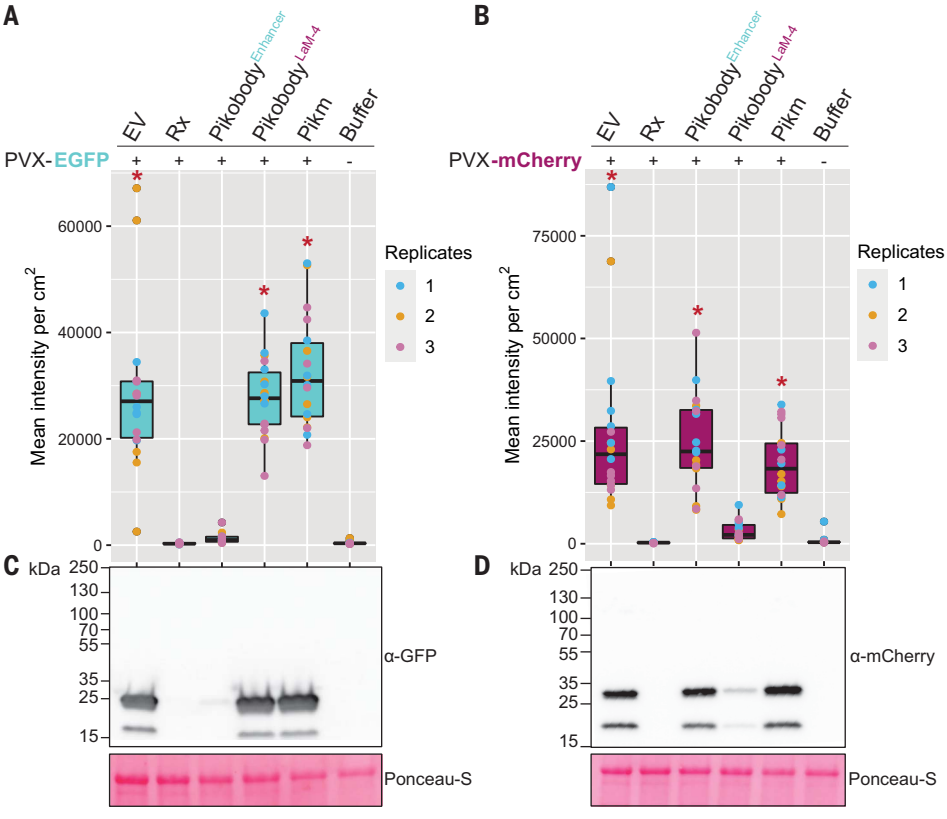

Fig. 2. Pikobodies confer resistance against PVX variants expressing matching FPs. (**A** and **B**) Specific reduction in fluorescence intensity of PVX-expressed EGFP or mCherry in the presence of Pikobody$^{\text{Enhancer}}$ or Pikobody$^{\text{LaM-4}}$, respectively. GFP (A) or mCherry (B) mean fluorescence intensity per square centimeter measured in *N. benthamiana* leaves 4 days after infiltration and used as a proxy for PVX viral load. Boxplots summarize results of three independent replicates with six internal replicates. Asterisks show significant differences between buffer only (no PVX added) and tested constructs in the presence of PVX-GFP (A) or PVX-mCherry (B) (Dunnett's test, $P < 0.001$). The PVX coat protein recognizing resistance protein Rx was used as a positive control for PVX resistance. (**C** and **D**) Specific reduction of PVX-expressed GFP (C) or mCherry (D) accumulation as a proxy to evaluate viral load in the presence of Pikobody$^{\text{Enhancer}}$ or Pikobody$^{\text{LaM-4}}$, respectively. Total protein was extracted 4 days after inoculation with PVX variants in the presence of the tested constructs and probed with the appropriate antibodies. Ponceau S staining shows equal protein loading across samples.

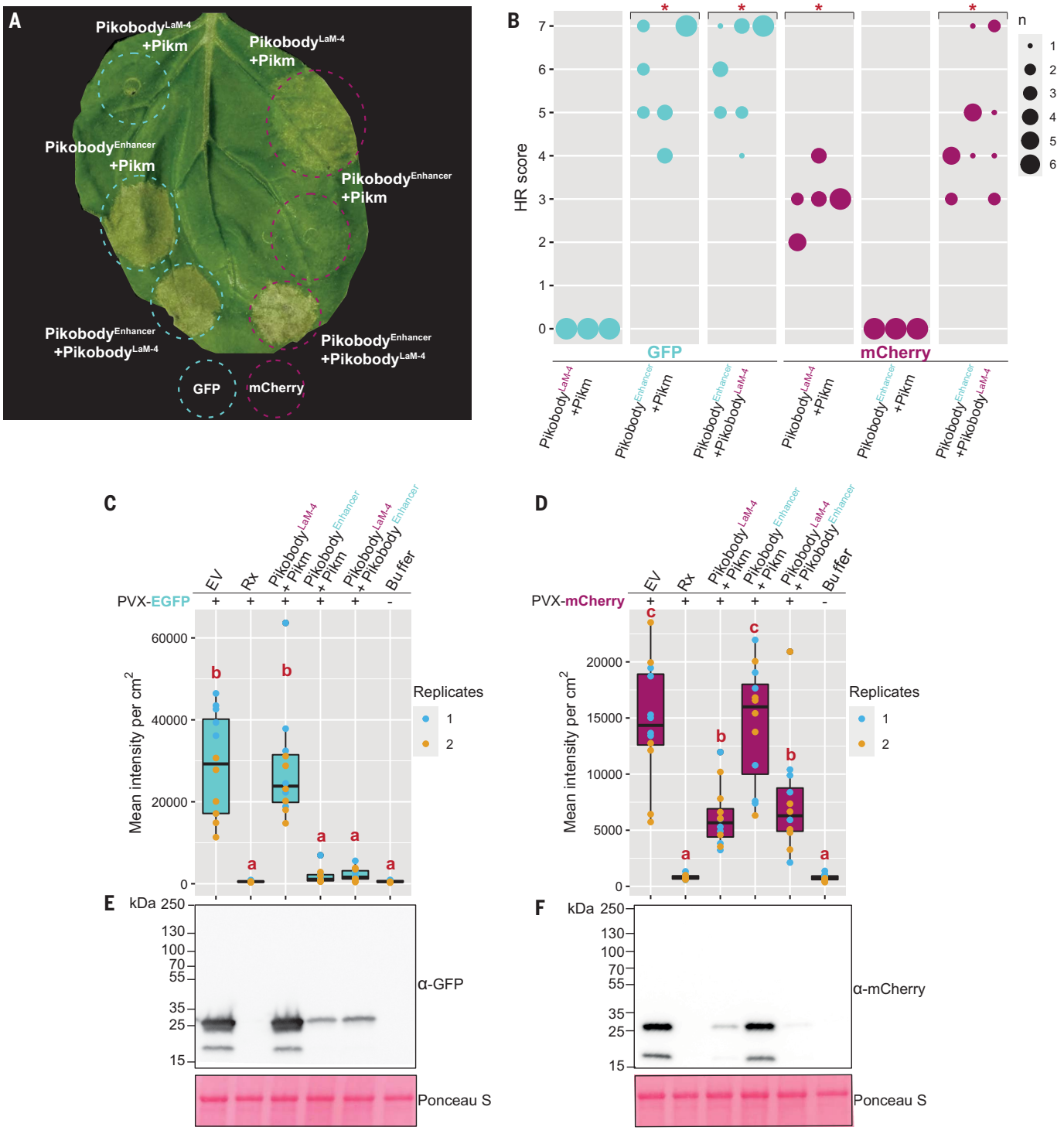

Fig. 3. Stacked Pikobodies result in additive immune recognition and disease resistance. (**A**) Pikobody stacking results in additive immune recognition. A representative *N. benthamiana* leaf infiltrated with indicated constructs is shown. Cyan or magenta dashed lines indicate GFP or mCherry coexpression, respectively. Leaves were photographed 4 days after infiltration. (**B**) HR quantification visualized as a dot plot, where the size of a dot is proportional to the number of samples with the same score (*n*) within the same replicate (1 to 3). The experiment was repeated three times with six internal replicates. Asterisks indicate statistically significant differences as compared with the Pikobody^{Enhancer}+Pikm+mCherry control, as determined by the besthr R package (*53*). (**C** and **D**) Specific reduction in fluorescence intensity of PVX-expressed GFP (C) and mCherry (D) in the presence of stacked Pikobody^{Enhancer} and Pikobody^{LaM-4}. Mean fluorescence intensity per square centimeter was measured in *N. benthamiana* leaves 4 days after infiltration and used as a proxy for PVX viral load. Boxplots summarize the results of three independent replicates with six internal replicates. Letters depict significant differences between treatments as determined by analysis of variance (ANOVA) followed by Tukey's honestly significant difference (HSD) test ($P < 0.05$). (**E** and **F**) Specific reduction of PVX-expressed GFP (E) or mCherry (F) accumulation as a proxy to evaluate viral load in the presence of stacked Pikobody^{Enhancer} or Pikobody^{LaM-4}. Total protein was extracted 4 days after inoculation with PVX variants in the presence of the tested constructs and probed with the appropriate antibodies. Ponceau S staining shows equal protein loading across samples.

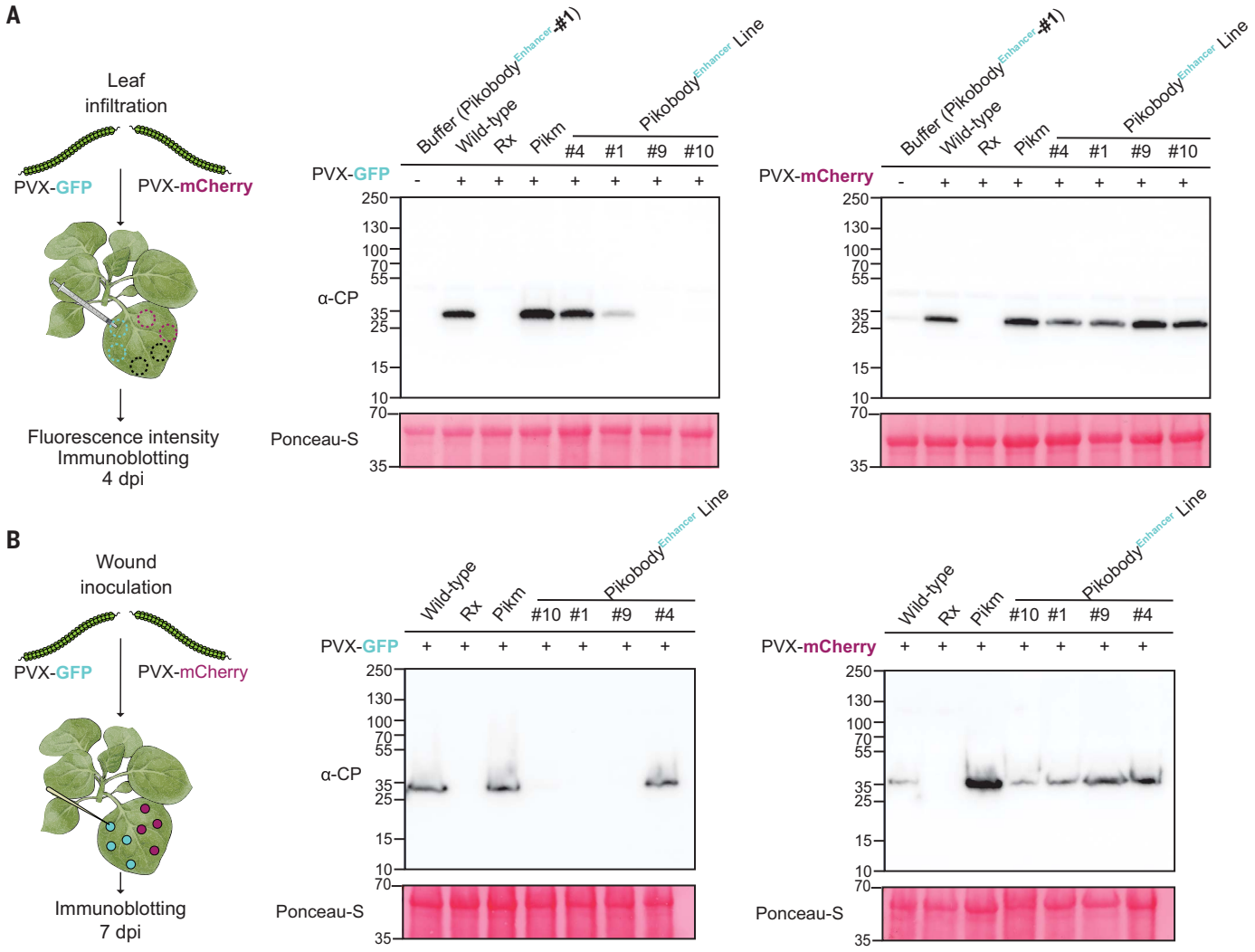

Fig. 4. Transgenic *N. benthamiana* Pikobody^{Enhancer} lines confer specific resistance to PVX-GFP. (**A**) Pikobody^{Enhancer} line 9 displays specific resistance to PVX-GFP—but not to PVX-mCherry—delivered by leaf agroinfiltration to an extent similar to that displayed by Rx. Coat protein (CP) accumulation was used to directly measure PVX viral load. For the immunoblot analysis, total protein was extracted 4 days after inoculation of the stated lines with PVX-GFP or PVX-mCherry and probed with the corresponding antibodies. Buffer only (no added PVX) was used as a negative control. Ponceau S staining shows equal protein loading across samples. dpi, days postinfiltration. (**B**) Pikobody^{Enhancer} lines 1 and 9 display specific resistance to PVX-GFP—but not to PVX-mCherry—delivered by wounding (toothpick inoculation of agrobacterium) to an extent similar to that of Rx. Immunoblot analysis is as in (A).

as the wild-type Pik pair (*36*) and other CC-NLRs. The conserved P-loop motif within the NB-ARC domain of CC-NLRs is required for the adenosine 5′-diphosphate (ADP)–adenosine 5′-triphosphate (ATP) switch that enables oligomerization into resistosome complexes (*37*, *38*). Pikobody^{K217R,Enhancer} and Pikobody$^{K217R,LaM-4}$ with a P-loop dead mutation in Pikm-2 (Pikm-2^{K217R}) failed to produce a HR to their corresponding FP even though the Pikm-1 and Pikm-2 proteins accumulated to similar levels as the wild-type immune receptors (fig. S4 and table S2). We conclude that the P-loop motif of Pikm-2 is required for Pikobody activity and that the Pikobody system probably functions through the established mechanistic model of NLRs (*39*).

Transient Pikobody expression confers immunity to PVX

Can Pikobodies produce a functional immune response that is effective against a pathogen? We used recombinant *Potato virus X* (PVX) (*40*) expressing either GFP or mCherry to assay the ability of Pikobodies to reduce viral load (table S1). These PVX variants express FPs from a duplicated coat protein subpromoter in the virus genome. We used fluorescence intensity and immunodetection of GFP or mCherry accumulation as proxy for viral load in leaf samples (Fig. 2 and table S3). Both Pikobody^{Enhancer} and Pikobody^{LaM-4} specifically reduced fluorescence intensity of PVX-expressed GFP or mCherry, respectively, to an extent comparable to that of Rx, an NLR known to confer immunity against PVX (*41*) (Fig. 2, A and B). This reduction of fluorescence intensity correlates with reduced accumulation of virus-expressed GFP or mCherry as compared with the empty vector control or wild-type Pikm (Fig. 2, C and D). We did, however, observe a faint signal corresponding to GFP or mCherry in the samples with PVX-GFP or PVX-mCherry and Pikobody^{Enhancer} or Pikobody^{LaM-4}, respectively, as compared with no detectable FP bands in the samples with Rx (Fig. 2, C and D).

To independently confirm these results, we tested two additional PVX variants expressing GFP from different virus genome locations (*42*, *43*) (tables S1 and S3 and fig. S5). Pikobody^{Enhancer} but not Pikobody^{LaM-4} reduced GFP fluorescence intensity and protein

accumulation when challenged with a PVX variant with the GFP sequence inserted between the triple gene block and coat protein in the virus genome (fig. S5, A and B). Furthermore, we observed reduced accumulation of virus-expressed GFP in the presence of Pikobody^{Enhancer} when challenged with a PVX variant carrying an in-frame N-terminal GFP fusion to the viral coat protein separated by a foot-and-mouth disease virus 2A self-cleaving peptide, despite consistently not seeing a significant change in fluorescence intensity in the presence of Pikobody^{Enhancer} (fig. S5, C and D). GFP fluorescence is known to be enhanced in the presence of certain nanobodies (*33*), and perhaps the fluorescent properties of the population of GFP that remains fused to the coat protein are enhanced under these conditions (*43*) (fig. S5D). Additionally, at late stages of infection Pikobody^{Enhancer} but not Pikobody$^{LaM\text{-}4}$ caused a visible HR with both variants of PVX-GFP (fig. S5, E and F).

We further compared the virus resistance capacity of Pikobody^{Enhancer} with the disease resistance protein Rx using PVX variants that contain mutations in the coat protein that evade Rx-mediated immunity (*44*). Unlike Rx, Pikobody^{Enhancer} conferred resistance against the Rx-evading variant PVX-GFP::CP^{T122K,M128R} (fig. S6 and table S3). We conclude that Pikobody^{Enhancer} can provide resistance against multiple PVX-GFP variants, including a variant that evades Rx.

Pikobody stacking results in additive recognition capacities

The addition of more than one immune receptor in a plant variety—a plant breeding strategy known as *R* gene stacking—can maximize resistance durability in the field by delaying the emergence of virulent pathogen races (*45*–*47*). However, coexpression of plant immune receptors can lead to autoimmunity (*48*, *49*) or suppression of recognition (*50*). We investigated whether Pikobodies with different FP specificities are compatible with each other (Fig. 3). We first determined that the coexpression of different Pikobodies does not result in autoimmunity or affect Pikobody accumulation (fig. S7 and table S2). Coexpression of Pikobody^{Enhancer} or Pikobody$^{LaM\text{-}4}$ and the wild-type Pikm pair triggered a HR only in the presence of the matching FP, whereas coexpression of Pikobody^{Enhancer} and Pikobody$^{LaM\text{-}4}$ produced a HR in the presence of both GFP and mCherry (Fig. 3, A and B). Similarly, coexpression of Pikobody^{Enhancer} and Pikobody$^{LaM\text{-}4}$ markedly reduced fluorescence intensity and protein levels of both GFP and mCherry produced by PVX-FPs (Fig. 3, C to F). At late stages of infection, the combination of Pikobody^{Enhancer} and Pikobody$^{LaM\text{-}4}$ also resulted in a HR in response to either PVX-GFP or PVX-mCherry (fig. S8). We conclude that Pikobody stacking can expand the recognition and response profile of these immune receptors without necessarily resulting in autoimmunity.

Transgenic plants expressing Pikobodies are resistant to PVX

We challenged our findings that Pikobodies confer virus resistance using stable *N. benthamiana* transgenic lines expressing Pikobody^{Enhancer} (Fig. 4). Among four lines transformed with Pikobody^{Enhancer}, three specifically respond to GFP, accumulate Pikm-2 and Pikm-1^{Enhancer} proteins, and reduce virus load of PVX-GFP but not of PVX-mCherry, as estimated by the accumulation of FPs and PVX coat protein (lines 1, 9, and 10) (fig. S9 and tables S4 and S5). A fourth transgenic that does not respond to GFP and only accumulates Pikm-2 protein and not Pikm-1^{Enhancer} protein served as a negative control (line 4) (Fig. 4 and fig. S10). The level of PVX resistance in one of the Pikobody^{Enhancer} transgenic lines (line 9) was similar to that of Rx, with no detectable levels of GFP and coat protein (Fig. 4 and fig. S10). Notably, the Pikobody^{Enhancer} transgenic lines conferred resistance to PVX regardless of the agroinfection method used to deliver the virus (leaf infiltration and wounding inoculation) (Fig. 4 and figs. S10 and S11). We conclude that transgenic Pikobody lines can confer specific resistance to PVX to a similar extent as the natural resistance gene Rx.

Discussion and conclusion

We built on our growing understanding of the evolution and function of the Pik pair of NLRs (*5*, *21*–*23*, *36*) to use Pik-1 as a chassis for VHH nanobody fusions to bioengineer functional disease resistance genes with new-to-nature functionalities. This strategy for bioengineering synthetic immune receptors differs from earlier approaches, which were based on the modification of endogenous sequences and domains. The Pikobody system provides a method to functionally transfer components of the metazoan immune system to plants. Given that Pikobodies rely on NLR-mediated immunity, this system shares the same limitations as other approaches that leverage this immune receptor family. For example, pathogen proteins will need to be translocated inside the plant cell during the right phase of pathogen infection to be recognized by Pikobodies. Nevertheless, given that nanobodies can be readily generated to bind virtually any antigen, Pikobodies have the potential to produce made-to-order resistance genes against any pathogen or pest that delivers effectors inside host plant cells (fig. S12).

REFERENCES AND NOTES

1. S. H. Kim, D. Qi, T. Ashfield, M. Helm, R. W. Innes, *Science* **351**, 684–687 (2016).
2. S. E. Pottinger *et al.*, *Mol. Plant Microbe Interact.* **33**, 932–944 (2020).
3. M. E. Segretin *et al.*, *Mol. Plant Microbe Interact.* **27**, 624–637 (2014).
4. A. Giannakopoulou *et al.*, *Mol. Plant Microbe Interact.* **28**, 1316–1329 (2015).
5. J. C. De la Concepcion *et al.*, *eLife* **8**, e47713 (2019).
6. S. Césari *et al.*, *Nat. Commun.* **13**, 1524 (2022).
7. S. Wang, W. Huang, Z. Duxbury, S. A. Hogenhout, J. D. G. Jones, bioRxiv 2021.09.06.459143 [Preprint] (2021). https://doi.org/10.1101/2021.09.06.459143.
8. J. L. Dangl, D. M. Horvath, B. J. Staskawicz, *Science* **341**, 746–751 (2013).
9. S. Césari, M. Bernoux, P. Moncuquet, T. Kroj, P. N. Dodds, *Front. Plant Sci.* **5**, 606 (2014).
10. C.-H. Wu, K. V. Krasileva, M. J. Banfield, R. Terauchi, S. Kamoun, *Front. Plant Sci.* **6**, 134 (2015).
11. T. Kroj, E. Chanclud, C. Michel-Romiti, X. Grand, J.-B. Morel, *New Phytol.* **210**, 618–626 (2016).
12. P. F. Sarris, V. Cevik, G. Dagdas, J. D. G. Jones, K. V. Krasileva, *BMC Biol.* **14**, 8 (2016).
13. S. Césari *et al.*, *Plant Cell* **25**, 1463–1481 (2013).
14. P. F. Sarris *et al.*, *Cell* **161**, 1089–1100 (2015).
15. C. Le Roux *et al.*, *Cell* **161**, 1074–1088 (2015).
16. A. Maqbool *et al.*, *eLife* **4**, e08709 (2015).
17. L. Guo *et al.*, *Proc. Natl. Acad. Sci. U.S.A.* **115**, 11637–11642 (2018).
18. T. K. Eitas, J. L. Dangl, *Curr. Opin. Plant Biol.* **13**, 472–477 (2010).
19. I. Ashikawa *et al.*, *Genetics* **180**, 2267–2276 (2008).
20. H. Kanzaki *et al.*, *Plant J.* **72**, 894–907 (2012).
21. J. C. De la Concepcion *et al.*, *Nat. Plants* **4**, 576–585 (2018).
22. J. C. De la Concepcion *et al.*, *PLOS Pathog.* **17**, e1009368 (2021).
23. A. Białas *et al.*, *eLife* **10**, e66961 (2021).
24. A. Białas *et al.*, *Mol. Plant Microbe Interact.* **31**, 34–45 (2018).
25. J. H. R. Maidment *et al.*, bioRxiv 2022.06.14.496076 [Preprint] (2022). https://doi.org/10.1101/2022.06.14.496076.
26. A. R. Bentham *et al.*, bioRxiv 2022.10.10.511592 [Preprint] (2022). https://doi.org/10.1101/2022.10.10.511592.
27. K. Yoshida *et al.*, *Plant Cell* **21**, 1573–1591 (2009).
28. C. Hamers-Casterman *et al.*, *Nature* **363**, 446–448 (1993).
29. A. S. Greenberg *et al.*, *Nature* **374**, 168–173 (1995).
30. S. Muyldermans, *Annu. Rev. Biochem.* **82**, 775–797 (2013).
31. D. Könning *et al.*, *Curr. Opin. Struct. Biol.* **45**, 10–16 (2017).
32. J. G. Dingus, J. C. Y. Tang, R. Amamoto, G. K. Wallick, C. L. Cepko, *eLife* **11**, e68253 (2022).
33. A. Kirchhofer *et al.*, *Nat. Struct. Mol. Biol.* **17**, 133–138 (2010).
34. P. C. Fridy *et al.*, *Nat. Methods* **11**, 1253–1260 (2014).
35. J. C. De la Concepcion *et al.*, *eLife* **10**, e71662 (2021).
36. R. Zdrzałek, S. Kamoun, R. Terauchi, H. Saitoh, M. J. Banfield, *PLOS ONE* **15**, e0238616 (2020).
37. J. Wang *et al.*, *Science* **364**, eaav5868 (2019).
38. S. P. Dinesh-Kumar, W.-H. Tham, B. J. Baker, *Proc. Natl. Acad. Sci. U.S.A.* **97**, 14789–14794 (2000).
39. F. L. W. Takken, W. I. L. Tameling, *Science* **324**, 744–746 (2009).
40. S. Marillonnet, C. Engler, V. Klimyuk, Y. Gleba, Potexvirus-derived replicon, Patent WO/2008/028661 (2008); https://patentscope.wipo.int/search/en/detail.jsf?docId=WO2008028661.
41. A. Bendahmane, K. Kanyuka, D. C. Baulcombe, *Plant Cell* **11**, 781–792 (1999).
42. R. Lu *et al.*, *EMBO J.* **22**, 5690–5699 (2003).
43. S. S. Cruz *et al.*, *Proc. Natl. Acad. Sci. U.S.A.* **93**, 6286–6290 (1996).
44. M. G. Goulden, B. A. Köhm, S. Santa Cruz, T. A. Kavanagh, D. C. Baulcombe, *Virology* **197**, 293–302 (1993).
45. M. Luo *et al.*, *Nat. Biotechnol.* **39**, 561–566 (2021).
46. S. Zhu, Y. Li, J. H. Vossen, R. G. F. Visser, E. Jacobsen, *Transgenic Res.* **21**, 89–99 (2012).
47. M. Ghislain *et al.*, *Plant Biotechnol. J.* **17**, 1119–1129 (2019).
48. E. Chae *et al.*, *Cell* **159**, 1341–1351 (2014).
49. D. T. N. Tran *et al.*, *Curr. Biol.* **27**, 1148–1160 (2017).
50. S. Hurni *et al.*, *Plant J.* **79**, 904–913 (2014).
51. Z. Zhang, Y. Wang, Y. Ding, M. Hattori, *Sci. Rep.* **10**, 6239 (2020).
52. Z. Wang *et al.*, *Protein Sci.* **30**, 2298–2309 (2021).
53. D. MacLean, besthr - Generating Bootstrap Estimation Distributions of HR Data, Github (2020); https://github.com/TeamMacLean/besthr.

ACKNOWLEDGMENTS

We thank the Tissue Culture and Transformation Team at the Sainsbury Laboratory for generating stable *N. benthamiana* transgenic lines containing the Pikobody system. We thank H. Pai for drawing the llama and the *N. benthamiana* plants in figs. S10 to S12, A. Białas for helpful comments on the figures, A. Williams for useful comments on the text, and P. Robinson for photography. We also thank our long-standing collaborators M. Banfield, N. Talbot, R. Terauchi, and other members of the BLASTOFF

community for the many useful discussions and suggestions. **Funding:** The authors received funding from the Gatsby Charitable Foundation (C.M., A.P., and S.K.), Biotechnology and Biological Sciences Research Council (BBSRC) BB/P012574 (Plant Health ISP) (S.K.), European Research Council (ERC) 743165 (A.H. and S.K.), and BASF Plant Science (J.K. and S.K.). The funders had no role in the study design, data collection and analysis, decision to publish, or preparation of the manuscript. **Author contributions:** Conceptualization: J.K., C.M., and S.K. Methodology: J.K. and C.M. Formal analysis: J.K., C.M., and A.P. Investigation: J.K., C.M., A.P., and A.H. Resources: J.K. Writing – original draft: J.K., C.M., and S.K. Writing – review & editing: J.K., C.M., A.P., A.H., and S.K. Visualization: J.K. and C.M. Supervision: S.K. Project administration: S.K. Funding acquisition: S.K. **Competing interests:** J.K., C.M., and S.K. receive funding from industry on NLR biology and have filed a patent on receptor-nanobody fusions (European patent application no. 21386064.6). The authors declare no other competing interests. **Data and materials availability:** Pikobody constructs generated for this study will be subjected to material transfer agreements (MTAs) and made available upon request. All data are available in the main text or the supplementary materials.

SUPPLEMENTARY MATERIALS

science.org/doi/10.1126/science.abn4116
Materials and Methods
Figs. S1 to S12
Tables S1 to S6
References (*54*–*64*)
MDAR Reproducibility Checklist

View/request a protocol for this paper from *Bio-protocol*.

Submitted 25 November 2021; resubmitted 9 December 2022
Accepted 1 February 2023
10.1126/science.abn4116